International Journal of Smart Grid and Clean Energy

Fabrication and enhanced electrochemical performances of MoO_3/graphene composite as anode material for lithium-ion batteries

Anjon Kumar Mondal*, Shuangqiang Chen, Dawei Su
Hao Liu, Guoxiu Wang

Centre for Clean Energy Technology, School of Chemistry and Forensic Science
University of Technology, Sydney, Broadway, Sydney, NSW 2007, Australia

Abstract

Molybdenum trioxide (MoO_3)/graphene composite were prepared by integrating MoO_3 and graphene in dimethylformamide (DMF). The morphology and structure of the materials were characterized by X-ray diffraction, field emission scanning electron microscopy and transmission electron microscopy. The electrochemical properties of MoO_3/graphene composite with different ratios were studied as anode materials for lithium-ion batteries using galvanostatic charge-discharge and cyclic voltammetry. We observed that the MoO_3/graphene anode with a weight ratio of 1:1 (MoO_3:graphene) exhibits a high lithium storage capacity of 967 mA h g^{-1} at the current density of 500 mA g^{-1}, satisfactory cycling stability and good rate capability.

Keywords: Lithium-ion battery, specific capacity, electrochemical properties, graphene, MoO_3 nanorods

1. Introduction

To meet the rising energy demands of modern electronic devices, lithium-ion batteries as energy storage devices for portable electronics and electric and hybrid electric vehicles, have attracted considerable attention in the scientific and industrial communities [1]-[3]. Graphite is used as anode material in the majority of commercial lithium-ion batteries due to its availability, and low cost, but the theoretical capacity is only 372 mA h g^{-1}, which cannot meet the ever rising demand for lithium-ion batteries with high capacity. Extensive studies have been devoted to develop new electrode materials for high energy applications. To achieve higher lithium storage capacities, different transition metal oxides have been widely investigated as anode materials for lithium-ion batteries [4]-[11]. Among various transition metal oxides MoO_3 has recently attracted much attention in lithium-ion batteries owing to its multiple valence states and high chemical and thermal stability [12]-[15]. However, this material also experience large volume variation during Li^+ insertion/extraction like other transition metal oxides. It is well established that the volume change causes pulverization of the electrode, which disconnect the active material from the substrate and subsequently lead to rapid loss of capacity. There are two methods to resolve these problems. One way is to reduce particle size into nanometer scale, because decrease in particle size leads to shorten the lithium-ion diffusion distance and enlarge the contact area between the active material and electrolyte [16], [17]. Another alternate is to prepare composites of oxides with carbon, which not only enhance the electronic conductivity of metal oxides but also prevent the exfoliation of active material from the substrate [18].

Graphene, a two-dimensional sp^2 bonded carbon atoms packed into a honeycomb crystal lattice, which exhibits many intriguing physical properties, such as a very high specific surface area, large electrical and

* Manuscript received June 15, 2013; revised July 30, 2013.
Corresponding author Tel.: +610295148244; *E-mail address*: Anjon.K.Mondal@student.uts.edu.au

thermal conductivity and mechanical flexibility [19]-[21]. In particular, the exceptionally high electron mobility is benificial for electrode. In metal oxide-graphene composite graphene layer can prevent both aggregation and volume changes of metal oxides during charge-discharge cycling and graphene can not restack because metal oxides are sandwiched in between the graphene sheets. Composites of graphene with different metal oxides have been reported and they have shown high specific capacity, good cycling performance and rate capability compared to the bulk metal oxides [22]-[26]. MoO_3-C composites have also been reported by several groups and achieved higher specific capacity and good cycling stability [27]-[29]. However, MoO_3/graphene composite with good electrochemical performances still remains limited.

In this work, we successfully prepared MoO_3 nanorods and graphene separately and fabricated MoO_3/graphene composite using DMF as solvent. The electrochemical properties of graphene-MoO_3 for lithium-ion batteries were systematically investigated and compared with the pure MoO_3.

2. Experimental

2.1. Preparation of MoO_3 nanorods

In a typical synthesis procedure, 0.49 g ammonium heptamolybdate tetrahydrate ($(NH_4)_6Mo_7O_{24}\cdot 4H_2O$) was dissolved in 15 ml de-ionised (DI) water and stirred for few mins. Then 8 mL of 3 M nitric acid was added into the above solution and stirred for 5 min. After stirring, 100 µl TX-100 was added slowly. The transparent solution was transferred into a Teflon-lined stainless autoclave and was heated to 180 $^{\circ}$C for 20 h. The resultant precipitate was collected, washed thoroughly with DI water and ethanol several times and dried at 80 $^{\circ}$C for 12 h.

2.2. Synthesis of graphene nanosheets

In a typical synthesis process, natural graphite powders were oxidized to graphite oxide using a modified Hummers method [30]. 1.0 g graphite powder and 0.5 g sodium nitrate were poured into 25 ml concentrated H_2SO_4 (under ice bath). 4.0 g $KMnO_4$ was gradually added and stirred for 2.5 h. The mixture was diluted with 150 ml de-ionised (DI) water. Then 5 % H_2O_2 was added into the solution until the colour of the mixture changed to brilliant yellow. The solution was washed with 5 % HCl and DI water until the pH=7. Then the obtained graphite oxide was dried in a vacuum oven overnight at 60 $^{\circ}$C. The dry graphite oxide was re-dispersed in DI water and exfoliated to generate graphene oxide nanosheets by ultrasonication using a Brandson Digital Sonifier. The brown graphene oxide nanosheet dispersion was poured into a round bottom flask and then 60 µl hydrazine monohydrate (reducing agent) was added into the dispersion. The mixed solution was then refluxed at 100 $^{\circ}$C for 3 h and the colour of the solution gradually changed to dark black as the graphene nanosheet dispersion was formed. The dispersion was then filtered and washed with DI water and ethanol and dried in vacuum oven at 60 $^{\circ}$C overnight to obtain bulk graphene nanosheets.

2.3. Preparation of MoO_3/graphene composite

Graphene nanosheets (30 mg) were dispersed in 50 ml DMF and sonicated by digital sonifier for 4 h. 30 mg MoO_3 nanorods were added in 50 ml DMF and sonicated in a bath sonifier for 30 min. The two dispersions were mixed by vigorous stirring. The mixture was filtered and washed with DI water and ethanol several times and dried in a vacuum oven at 80 $^{\circ}$C overnight. Three composites were prepared with the weight ratios of graphene: MoO_3 equal 1:3, 1:1, and 3:1.

2.4. Materials characterization

The as-prepared materials were characterized by GBC MMA X-ray diffractometer (λ=0.15405 nm), field emission scanning electron microscopy (FESEM, Zeiss Supra 55VP) and transmission electron microscopy (TEM, JEOL 2011 TEM facility).

2.5. Electrochemical measurements

Electrochemical measurement of the material was carried out using CR 2032 coin type cells. The working electrodes were prepared by mixing active materials (MoO_3/graphene composite and MoO_3) acetelene black and the binder in a weight ratio of 70:20:10 in N-methyl-2-pyrrolidinone (NMP) solvent. Polyvinylidene fluoride (PVDF) was used as binder. The slurry was then pasted uniformly on a copper-foil substrate and then dried in a vacuum oven at 100 $^{\circ}$C for 12 h. 1 M $LiPF_6$ solution dissolved in a solvent mixture, which contain 50 vol % of ethylene carbonate and 50 vol % of dimethyl carbonate (1:1 by volume) as electrolyte. The cells were assembled in a high purity argon-filled glove box (UniLab, MBRAUN, Germany) using lithium foil as both counter electrode and reference electrode. Galvanostatic charge-dischage tests were performed using Neware battery tester within the potential window of 0.01-3.0 V. Cyclic voltammetry measurements were performed using a CHI 660C electrochemistry workstation at a scan rate of 0.1 mV s^{-1} in the potential range of 0.01-3.0 V.

3. Results and Discussion

The XRD patterns of the MoO_3 nanorods and MoO_3/graphene composite are shown in Fig. 1. As shown in Fig. 1 (a) all the diffraction peaks can be indexed to an orthorhombic phase of MoO_3 (JCPDS 35-0609). No other peaks related to impurities were observed, indicating that pure α-MoO_3 was obtained. From the XRD pattern (Fig. 2 (b)) of MoO_3/graphene composite (1:1 in weight ratio), it can be seen that the absorption peaks of MoO_3 are also exhibited in the composite, which indicate MoO_3 nanorods were also formed on the surface of graphene sheets.

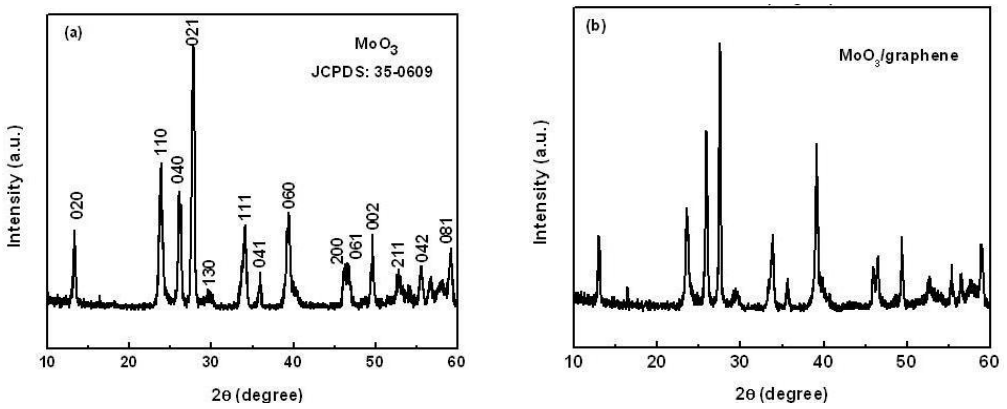

Fig. 1. XRD patterns of as-prepared (a) MoO_3 nanorods and (b) MoO_3/graphene composite (1:1 in weight ratio).

FESEM was employed to observe the morphology of the MoO_3/graphene composite (1:1 in weight ratio). From the low magnification images (as shown in Fig. 2 (a) and (b)) we can see the uniform distribution of graphene and MoO_3 nanorods. The higher magnification FESEM observation (Fig. 2 (c) and (d)) clearly indicates that the MoO_3 nanorods well penetrated into the graphene matrix.

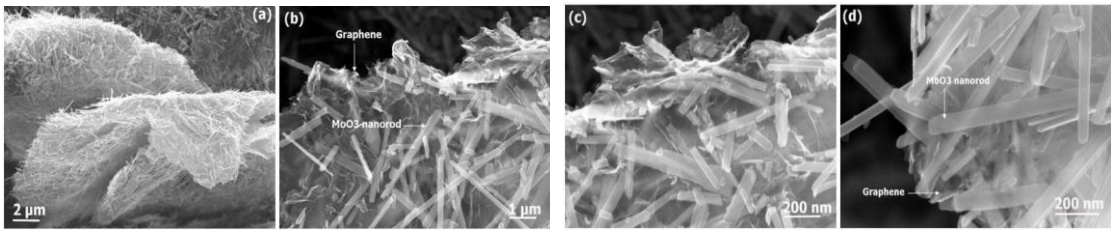

Fig. 2. FESEM images of MoO_3/graphene composite (1:1 in weight ratio) (a) and (b) low magnification and (c) and (d) high magnification.

Fig. 3 shows the TEM images of MoO_3/graphene composite. From the low and high magnification images (as shown in Fig 3 (a) and (b)) it can be observed clearly that the MoO_3 nanorods and graphene homogeneously mixed in the composite.

The charge-discharge curves of the MoO_3/graphene composite electrode (1:1 in weight ratio) for the 1st, 2nd, 50th and 100th cycles at a current density of 500 mAg^{-1} is shown in Fig. 4. The subsequent discharge capacities are 1437, 967, 688 and 574 $mAhg^{-1}$, respectively. The initial extra discharge capacity could be attributed to the formation of the solid electrolyte interface (SEI) layer, which can efficiently protect the electrode from the intercalation of solvent in the subsequent cycles [31], [32]. The capacity versus cycle number of the MoO_3/graphene composite electrode is presented in Fig. 4 (b). The electrode still maintains the reversible capacity of 574 mA hg^{-1} after 100 cycles at the current density of 500 mAg^{-1}. The electrode shows an average Coulombic efficiency of 97 % from the second cycle.

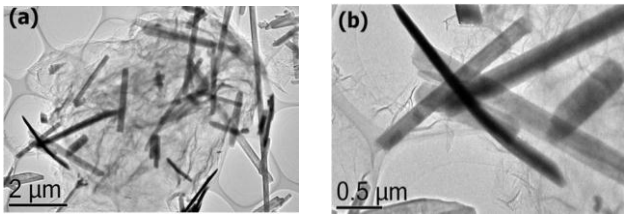

Fig. 3. TEM images of MoO_3/graphene composite (1:1 in weight ratio) (a) low magnification (b) high magnification.

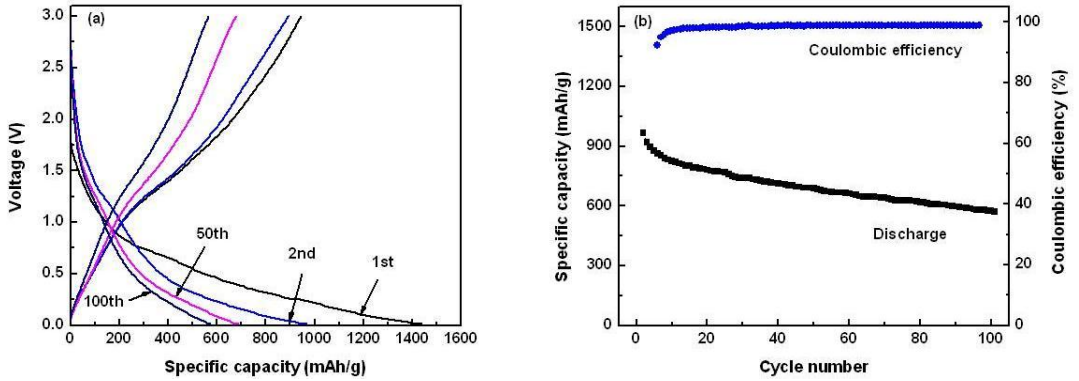

Fig. 4. (a) Galvanostatic charge-discharge curves for the 1st, 2nd, 50th and 100th cycles and (b) cycling performance and Coulombic efficiency of MoO_3/graphene composite electrode (1:1 in weight ratio) at a current density of 500 mA g^{-1} in the potential range of 0.01-3.0 V.

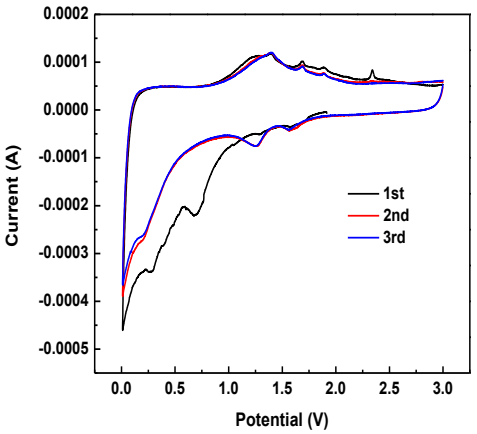

Fig. 5. CV curves of the MoO_3/graphene composite electrode (1:1 in weight ratio) for the first three cycles at the scan rate of 0.1 mVs^{-1} in the potential range of 0.01-3.0 V vs. Li/Li^+.

The CV curves of the MoO_3/graphene composite (1:1 in weight ratio) for first 3 cycles are shown in Fig. 5. Two irreversible cathodic peaks at 0.67 and 0.27 V was observed in the first cycle corresponds to the reduction of electrolyte solution and formation of solid electrolyte interface (SEI) layer on the surface of working electrode, which disappears in the following cycles [33]. In the first cycle two anodic peaks at 1.22 and 2.34 V was also observed which are due to the extraction process of lithium from its oxides. In the subsequent cycles two redox couples are well overlapped, indicating good reversibility for lithium ion intercalation and de-intercalation.

The MoO_3/graphene composite electrode (1:1 in weight ratio) was cycled stepwise under four different current densities to investigate the rate performance. Six cycles for each current density were carried out in the potential range of 0.01-3.0 V. As shown in Fig. 6 the composite electrode delivered the discharge capacities of 1018,734,597 $mAhg^{-1}$ at the current densities of 100,300 and 600 mAg^{-1}, respectively. The electrode still delivered the capacity of 513 $mAhg^{-1}$ even at a high current density of 1000 mAg^{-1} which reveals the good rate capability of the composite. When the current density back to the 500 mAg^{-1} and 100 mAg^{-1} the capacities of the electrode can recover to the high values, which indicates that the composite electrode is tolerant to the high current charge/discharge.

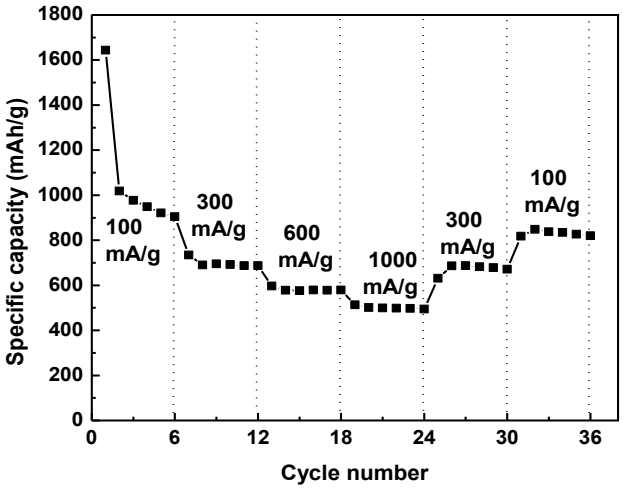

Fig. 6. Rate performances of the MoO_3/graphene composite electrode (1:1 in weight ratio) between 0.01 and 3.0 V at different current densities.

The cycling performances of the MoO_3/graphene composite at different ratios and neat MoO_3 electrodes at the current density of 500 mAg^{-1} in the voltage range of 0.01-3.0 V are presented in Fig. 7. MoO_3/graphene composite at different ratios shows higher specific capacity and better cycling stability compared to neat MoO_3. The reversible capacity of MoO_3 electrode decreases from 926 $mAhg^{-1}$ to 190 $mAhg^{-1}$ at the current density of 500 mAg^{-1} after 100 cycles. On the contrary, MoO_3/graphene composite shows the reversible capacities of 309, 373, and 574 $mAhg^{-1}$ at the ratios of 1:3, 3:1 and 1:1, respectively after 100 cycles. During lithium intercalation MoO_3 electrode experience pulverization and cracking problem during charge and discharge cause the rapid capacity loss of the electrode [34]. Although the capacities of MoO_3/graphene composite in different ratios decreases fast up to 20 cycles but they reaches a steady status in the subsequent cycles. The enhanced performance in the subsequent cycles can be ascribed to the unique structure of the composite and existence of graphene. Graphene provides electronic conduction and can accommodate the volume expansion of MoO_3 during charge-discharge, maintain the structural integrity and therefore, improve the cycling performance of the electrode. Meanwhile, MoO_3 nanorods dispersed in graphene sheets in certain extent prevent graphene sheet from re-stacking in the composite.

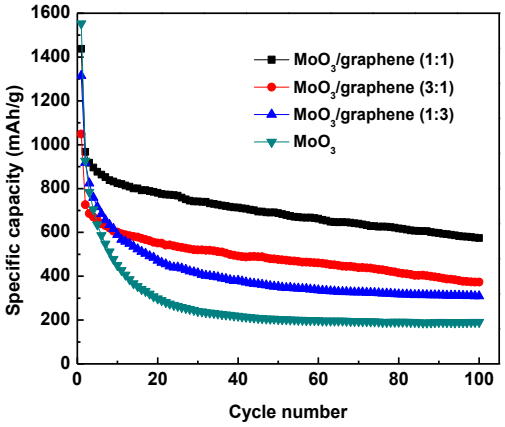

Fig. 7. Cycling performance of MoO_3 and MoO_3/graphene composite (at different ratios)

The optimization of MoO_3 and graphene ratio is also important for improving the electrochemical performance. As shown in Fig. 7 MoO_3/graphene composite with the weight ratio of 1:1 showed better cycling stability than other two ratios. The specific capacity decreased in the MoO_3/graphene composite (1:3 in weight ratio) because less amount of MoO_3 is used, which is not sufficient to prevent aggregation of graphene sheets. The low percentage of graphene (3:1 in weight ratio) resulted in less spaces to anchor MoO_3, which can not accommodate the large volume expansion of MoO_3 nanorods during cycling, which results in the decrease of specific capacity. Both graphene and MoO_3 nanorods in the weight ratio of 1:1 shows a strong synergistic effect in the composite and therefore enhance the cycling performance.

4. Conclusions

In this article, we report a facile strategy to fabricate MoO_3/graphene composite as an anode material for lithium-ion batteries. The obtained MoO_3/graphene composite (1:1 in weight ratio) exhibited high lithium storage capacity and cycling stability relative to 1:3 and 3:1 ratios and the neat MoO_3 nanorods. MoO_3/graphene composite (1:1 in weight ratio) still shows the specific capacity of 574 $mAhg^{-1}$ at the current density of 500 mAg^{-1} after 100 cycles. The results suggest that MoO_3/graphene composite could be a promising anode material for lithium-ion batteries.

Acknowledgements

The authors gratefully acknowledge the financial support provided by the Australian Research Council (ARC) through the ARC discovery project (DP1093855) and Chinese Scholar Council (CSC) (No. 2011689009).

References

[1] Tollefson J. Car industry: charging up the future. Nature, 2008; 456(7221): 436-440.
[2] Scrosati B. Battery technology-challenge of portable power. Nature, 1995; 373(6515): 557-558.
[3] Kang B, Ceder G. Battery materials for ultrafast charging and discharging. Nature 2009; 458(7235): 190-193.
[4] Poizot P, Laruelle S, Grugeon S, Dupont L, Tarascon JM. Nano-sized transition-metal oxides as negative-electrode materials for lithium-ion batteries. Nature 2000; 407(6803) 496-499.
[5] Lou XW, Deng D, Lee JY, Archer LA. Thermal formation of mesoporous single-crystal Co(3)O(4) nano-needles and their lithium storage properties. J. Mater. Chem. 2008; 18(37): 4397-4401.
[6] Zhao NH, Wang GJ, Huang Y, Wang B, Yao BD, Wu YP. Preparation of nanowire arrays of amorphous carbon nanotube-coated single crystal SnO_2. Chem. Mater. 2008; 20(8): 2612-2614.
[7] Ni S, Li T, Yang X. Fabrication of NiO nanoflakes and its application in lithium ion battery. Mater. Chem. Phys. 2012; 132(2-3): 1108-1111.

[8] Yang LC, Gao QS, Zhang YH, Tang Y, Wu YP. Tramella-like molybdenum dioxide consisting of nanosheets as an anode material for lithium ion battery. Electrochem. Commun. 2008; 10(1): 118-122.
[9] Hu YS, Kienle L, Guo YG, Maier J. High lithium electroactivity of nanometer-sized rutile TiO_2. Adv. Mater. 2006; 18(11): 1421-1426.
[10] Kim H, Cho J. Hard templating synthesis of mesoporous and nanowire SnO_2 lithium battery anode materials. J. Mater. Chem. 2008; 18(7): 771-775.
[11] Zhang J, Huang T, Liu Z, Yu A. Mesoporous Fe_2O_3 nanoparticles as high performance anode materials for lithium-ion batteries. Electrochem. Commun. 2013; 29: 17-20.
[12] Chen JS, Cheah YL, Madhavi S, Lou XW. Fast synthesis of alpha-MoO_3 nanorods with controlled aspect ratios and their enhanced lithium storage capabilities. J. Phys. Chem. C, 2010; 114(18): 8675-8678.
[13] Chernova NA, Roppolo M, Dillon AC, Whittingham MS. Layered vanadium and molybdenum oxides: batteries and electrochromics. J. Mater. Chem. 2009; 19(17): 2526-2552.
[14] Zhou L, Yang L, Yuan P, Zou J, Wu Y, Yu C. α-MoO_3 Nanobelts: A high performance cathode material for lithium ion batteries. J. Phys. Chem. C 2010; 114(49): 21868-21872.
[15] Mai LQ, Chen W, Xu Q, Zhu QY. Effect of modification by poly(ethylene-oxide) on the reversibility of Li insertion/extraction in MoO_3 nanocomposite films, Microelectron. Eng. 2003; 66(1-4): 199-205.
[16] Bruce PG, Scrosati B, Tarascon JM. Nanomaterials for rechargeable lithium batteries. Angew. Chem. Int. Ed. 2008; 47: 2930-2946.
[17] Ji L, Lin Z, Alcoutlabi M, Zhang X. Recent developments in nanostructured anode materials for rechargeable lithium-ion batteries. Energy Environ. Sci. 2011; 4(8): 2682-2699.
[18] Huiqiao L, Zhou H. Enhancing the performances of Li-ion batteries by carbon-coating: present and future. 2012; 48(9): 1201-1217.
[19] Geim AK, Novoselov KS. The rise of graphene. Nat. Mater. 2007; 6(3): 183-191.
[20] Zhang YB, Tan YW, Stormer HL, Kim P. Experimental observation of the quantum Hall effect and Berry's phase in graphene. Nature 2005; 438(7065): 201-204.
[21] Novoselov KS, Geim AK, Morozov SV, Jiang D, Zhang Y, Dubonos SV, Grigorieva IV, Firosov AA. Electric field effect in atomically thin films. Science 2004; 306(5696): 666-669.
[22] Mai YJ, Shi SJ, Zhang D, Lu Y, Gu CD, Tu JP. NiO-graphene hybrid as an anode material for lithium ion batteries. J. Power Sources 2012; 204: 155-161.
[23] Mai YJ, Zhang D, Qiao YQ, Gu CD, Wang XL, Tu JP. MnO/reduced graphene oxide sheet hybrid as an anode for Li-ion batteries with enhanced lithium storage performance. J. Power Sources 2012; 216: 201-207.
[24] Zhu X, Zhu Y, Murali S, Stoller MD, Ruoff RS. Nanostructured reduced graphene oxide/Fe_2O_3 composite as a high-performance anode material for lithium ion batteries. ACS Nano 2011; 5(4): 3333-3338.
[25] Li B, Cao H, Shao J, Li G, Qu M, Yin G. Co_3O_4@graphene composites as anode materials for high-performance lithium ion batteries. Inorg. Chem. 2011; 50(5): 1628-1632.
[26] Zhang LS, Jiang LY, Yan HJ, Wang WD, Wang W, Song WG, Guo YG. Mono dispersed SnO_2 nanoparticles on both sides of single layer graphene sheets as anode materials in Li-ion batteries. J. Mater. Chem. 2010; 20(26): 5462-5467.
[27] Hassan MF, Guo JP, Chen Z, Liu HK. Carbon-coated MoO_3 nanobelts as anode materials for lithium-ion batteries. J. Power Sources 2010; 195(8): 2372-2376.
[28] Riley LA, Lee S-H, Gedvilias L, Dillon AC. Optimization of MoO_3 nanoparticles as negative-electrode material in high-energy lithium ion batteries. J. Power Sources 2010; 195(2): 588-592.
[29] Tao T, Glushenkov AM, Zhang CF, Zhang HZ, Zhou D, Guo ZP, Liu HK, Chen QY, Hu HP, Chen Y. MoO_3 nanoparticles dispersed uniformly in carbon matrix: a high capacity composite anode for Li-ion batteries. J. Mater. Chem. 2011; 21(25): 9350-9355.
[30] Hummers WS, Offeman RE. Preparation of graphitic oxide. J. Am. Chem. Soc. 1958; 80(6): 1339.
[31] Débart A, Dupont L, Poizot P, Leriche JB, Tarascon JM. A Transmission Electron Microscopy Study of the Reactivity Mechanism of Tailor-Made CuO Particles toward Lithium. J. Electrochem. Soc. 2001; 148(11): A1266-A1274.
[32] Liu H, Wang GX, Liu J, Qiao SZ, Ahn H. Highly ordered mesoporous NiO anode material for lithium ion batteries with an excellent electrochemical performance. J. Mater. Chem. 2011; 21(9): 3046-3052.
[33] Itagaki M, Yotsuda S, Kobari N, Watanabe K, Kinoshita S, Ue M. Electrochemical impedance of electrolyte/electrode interfaces of lithium-ion rechargeable batteries-effect of additives to the electrolyte on negative electrode. Electrochim. Acta 2006; 51(8-9): 1629-1635.
[34] Dillon AC, Riley LA, Jung YS, Ban C, Molina D, Mahan AH, Cavanagh AS, George SM, Lee S-H. HWCVD MoO_3 nanoparticles and a-Si for next generation Li-ion anodes. Thin Solid Films 2011; 519(14): 4495-4497.